Proposal for Nuclear Physics Experiment at RI Beam Factory
(RIBF NP-PAC-01, 2007)

Title of Experiment :   Studies of Exotic Nuclei using (p,2p) Proton Knockout Reactions

and

Construction of a Broad-Range Magnetic Spectrometer

[X]   NP experiment   [   ] Detector R&D   [   ]   Construction

Spokesperson :

Name   T. Kobayashi   /   R.C. Lemmon   /   A.S. Fomichev

Institution   Dep. of Physics, Tohoku Univ.   /   CCLRC Daresbury Lab.   /   JINR

Title of position   prof.   /   staff scientist   /   research group leader

Address   Aoba, Aramaki, Aoba, Sendai 980-8578, Japan

Keckwick Lane, Daresbury, Warrington, Cheshire, WA4 4AD, United Kingdom

Dubna, 141980, Russia

TEL : 81-22-795-6448   FAX : 81-22-795-6455   Email : kobayash@lambda.phys.tohoku.ac.jp

TEL : 00 44 (0) 1925 603926   FAX : 00 44 (0) 1925 603173   Email : r.c.lemmon@dl.ac.uk

TEL : 7 496 216 4544   FAX : 7 496 216 5083   Email : fomichev@nrmail.jinr.ru

Experimental Device:

[X]   BigRIPS

Beam Time Request Summary

Tuning with beam	8h x 6	Hours
DATA RUNS 12(p)+40(He)+53(Li)+50(C)+65(O)+10(Ne)		Hours
Total	**278**	**Hours**

Primary Beam

Particle	^{18}O	Energy	350	(A MeV)	Intensity	<200pnA
Particle	^{22}Ne	Energy	350	(A MeV)	Intensity	<200pnA
Particle	^{48}Ca	Energy	350	(A MeV)	Intensity	<200pnA
Particle	^{20}Ne	Energy	400	(A MeV)	Intensity	<200pnA

Sheet for an experiment with RI beam

[X]   BigRIPS

RI Beams			Beam-On-Target Time for DATA RUN
Isotope (primary)	Energy (MeV/A)	Intensity (/s)	hours/days
p (^{18}O)	~270	~10^6	12 h
$^{3,4,6,8}He$ (^{18}O)	~250	~$3x10^5$	10 h x 4 = 40 h
$^{6,7,8,9}Li$ (^{18}O)	~250	~$3x10^5$	10 h x 4 = 40 h
^{11}Li (^{18}O)	~250	~$2.4x10^5$	13 h x 1 = 13 h
$^{14,15,16,17,18}C$ (^{22}Ne)	~250	~$3x10^5$	10 h x 5 = 50 h

^{1921}F (^{22}Ne)	~250	~3x10^5	10 h x 2 = 20 h
^{2324}F (^{48}Ca)	~250	~3x10^5	10 h x 2 = 20 h
^{25}F (^{48}Ca)	~250	~1.2x10^5	25 h
^{17}Ne (^{20}Ne)	~250	~3x10^5	10 h

Estimated date ready to run the experiment   <u>**winter 2007 (except forward magnetic spectrometer)**</u>

Dates which should be excluded, if any   _____

Summary of Experiments

Firstly, we propose to construct a broad-range magnetic spectrometer utilizing a secondhand C-type magnet with moderate bending power (BL= 2.2 Tm) and gap (40cm).   This is one of the missing facilities at RIBF.   The magnetic spectrometer will be used to measure the decay mode of the hole states produced in the (p,2p) reaction.

We propose to study light exotic nuclei using (p,2p) proton knockout reactions at 250 MeV/A on the following three subjects:

(1) Charge radius of the inner shell for He, Li, and C isotopes will be studied using He,Li,C(p,2p) reactions by measuring momentum distributions of strongly-bound inner-shell (1s) protons.

(2) Spectroscopic studies of Oxygen isotopes around the new magic number N=16, including the particle-unbound states in the doubly-magic nucleus ^{24}O, will be performed using F(p,2p)O reactions.

(3) Proton-rich nucleus ^{17}Ne will be studied using ^{17}Ne(p,2p) reaction by measuring the momentum distribution of weakly-bound valence protons in the 2s/1d orbit.

List of Collaborators

Name	institution	Title or position	Email
T. Kobayashi	Tohoku Univ.	prof.	kobayash@lambda.phys.tohoku.ac.jp
K. Ozeki	Tohoku Univ.	res. associate	ozeki@he4.phys.tohoku.ac.jp
K. Maeda	Tohoku Univ.	associate prof.	maeda@mail.tains.tohoku.ac.jp
T. Tamae	Tohoku Univ.	associate prof.	tamae@lns.tohoku.ac.jp
N. Chiga	Tohoku Univ.	engineer	chiga@lambda.phys.tohoku.ac.jp
Y. Matsuda	Tohoku Univ.	grad. student, D3	matsuda@he4.phys.tohoku.ac.jp
E. Takada	NIRS	head	takada@nirs.go.jp
H. Sakaguchi	Miyazaki Univ.	prof.	sakaguti@phys.miyazaki-u.ac.jp
T. Noro	Kyushu Univ.	prof.	noro@nucl.phys.kyushu-u.ac.jp
H. Otsu	RIKEN	senior research scientist	otsu@ribf.riken.jp
H. Takeda	RIKEN	res. associate	takeda@ribf.riken.jp
S. Terashima	RIKEN	res. associate	tera@ribf.riken.jp
Y. Sato	Tokyo Inst. Tech.	rea. associate	satou@phys.titech.ac.jp
R.C. Lemmon	Daresbury Lab.	staff scientist	r.c.lemmon@dl.ac.uk
M. Labiche	Daresbury Lab.	staff scientist	m.labiche@dl.ac.uk
M. Chartier	Liverpool Univ.	lecturer	mc@ns.ph.liv.ac.uk
B. Fernandez-Dominguez	Liverpool Univ.	res. associate	bfd@ns.ph.liv.ac.uk
W. Catford	Surry Univ.	reader	w.catford@surrey.ac.uk
T. Aumann	GSI	staff scientist	t.aumann@gsi.de
O. Kiselev	GSI	staff scientist	o.kiselev@gsi.de
P. Egelhof	GSI	staff scientist	p.egelhof@gsi.de
W.Mittig	GANIL	Prof.	mittig@ganil.fr
L.Gaudefroy	GANIL	Dr.	gaudefroy@ganil.fr
N.Orr	LPC-Caen	Dr.	orr@lpccaen.in2p3.fr
A.S. Fomichev	JINR	group leader	fomichev@nrmail.jinr.ru
G.M. Ter-Akopian	JINR	chief scientist	Gurgen.TerAkopian@jinr.ru
M.S. Golovkov	JINR	senior scientist	golovkov@nrmail.jinr.ru
S.A. Krupko	JIMR	engineer	krupko@nrmail.jinr.ru
A.M. Rodin	JINR	senior scientist	rodin@nrmail.jinr.ru

S.I. Sidorchuk	JINR	senior scientist	sid@nrmail.jinr.ru
S.V. Stepantsov	JINR	senior scientist	stepantsov@nrmai.jinr.ru
R. Wolski	JINR	leading scientist	wolski@nrmail.jinr.ru

Studies of Exotic Nuclei Using (p,2p) Proton Knockout Reactions

and Construction of a Broad-Range Magnetic Spectrometer

[1] **Introduction**

Nucleon knockout (p,pN) reactions are among the most direct experimental techniques to study single-particle properties of nuclei such as the separation energy, momentum distribution, angular momentum, and spectroscopic factors, of bound nucleons in the nucleus, as demonstrated for stable nuclei using proton beams [1]. This method can be used to study the single-particle properties of both valence and inner-shell orbits because of the usage of a proton beam. In inverse kinematics, the bound nucleon in the projectile is knocked out via quasifree NN scattering with a proton target, and a hole state is produced as a residual nucleus. By measuring the 4-momenta of the two nucleons in the final state, the separation energy (S_p) and momentum ($\vec{q}$) of the knocked out nucleon are obtained. Since the hole state is produced with the beam velocity, the decay modes of the hole state can be measured with high efficiency by detecting the hole state itself or particles from the decay of the hole state in the forward direction. For the reaction to be quasifree, the beam energy needs to be relatively high, and thus this type of reaction is ideally suited for the beam energies available at RIBF.

Nucleon knockout reactions using nuclear targets such as Be, where the excited states are tagged by γ-rays, have been extensively studied at MSU and GSI [8]. Momentum distributions are measured by high-resolution magnetic spectrometers for identifying the angular momentum and spectroscopic factors for the ground and excited states are then deduced. Compared with this method, nucleon knockout (p,pN) reactions using a hydrogen target generally suffer from worse separation energy resolution since only the outgoing nucleons are measured, but have several merits such as the sensitivity to the nuclear interior or inner shells, the applicability to particle-unbound final states and better control of the final state interactions.

In this proposal, we concentrate on three specific subjects using high-intensity RI beams : (1) charge radius measurements for He, Li, and C isotopes, related to single-particle properties of inner-shell orbits in light nuclei, (2) spectroscopic studies of Oxygen isotopes around the new magic number N=16, related to the study of unbound final states, and (3) studies of [17]Ne, the candidate for a two-proton halo. Although conventional detectors with relatively small solid angles are employed in the present measurements, we intend to upgrade the detectors in the future by constructing a target recoil detector array which will combine a tracking detector composed of multiple layers of double-sided silicon microstrip and/or MAPS detectors, and a calorimeter detector composed of scintillating crystals such as CsI. This will allow us to cover larger solid angles and so extend the measurements to weaker RI beams.

[2] **Motivation and Goals**

(2-1) **Motivation**

We have performed (p,2p) experiments on $^{9-16}$C isotopes using 250 MeV/A RI beams at HIMAC/NIRS, for studying deeply (20-50MeV)-bound inner-shell protons in the $1s_{1/2}$ orbit as well as weakly (1.3MeV)- to strongly (22.3MeV)-bound valence protons in the $1p_{3/2}$ orbit. One of the interesting observations is that the charge rms radius of the $1s_{1/2}$ orbit is shrinking, possibly with a zigzag pattern, from 2.0 fm for ^{9}C down to 1.5 fm for ^{16}C, as shown in Fig. 1. The rms charge radius is deduced from the Fourier transform of the momentum distribution of the 1s protons, assuming harmonic oscillator wave functions. The behavior of the charge radius is different from that predicted by a simple potential model with adjustable separation energy or that predicted by a standard RMF model, both of which give a rather constant charge radius for the 1s orbit. We think that the (p,2p) reaction can be used to study systematically the charge radius of the core, in which protons are very strongly bound especially in neutron-rich nuclei. This method may give new information on the modification of the core in neutron-rich nuclei.
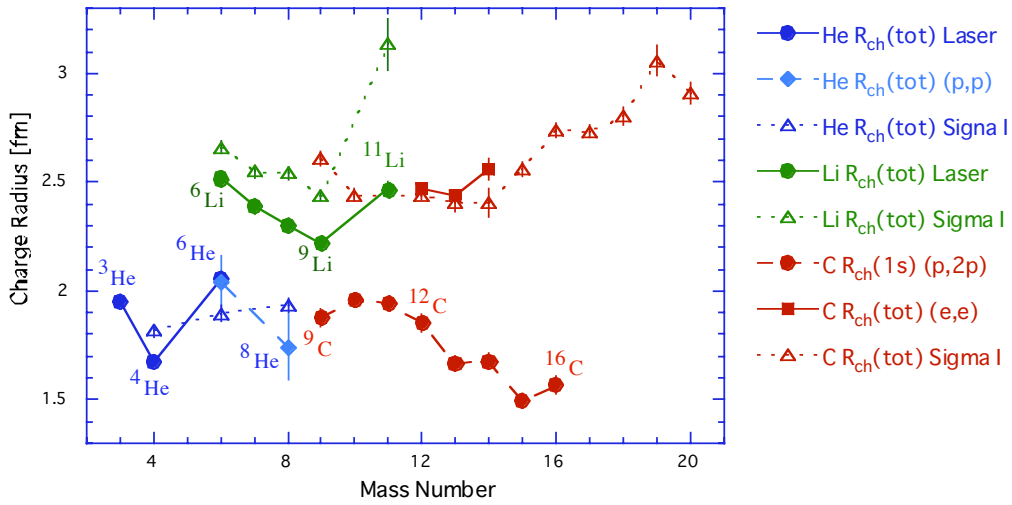

Fig. 1 : Charge radii of He, Li, and C isotopes

Charge radii of light unstable nuclei have been deduced from interaction cross-section measurements [2,3] and proton elastic scattering measurements [4]. Direct charge radius measurements for $^{3-6}$He [5] and $^{6-11}$Li [6] isotopes have been performed using laser spectroscopy. These data are also shown in Fig. 1. For He isotopes, the charge radius increases from ^{4}He to ^{6}He, and σ_I and (p,p) measurements give different behavior for ^{8}He. For Li isotopes, the charge radius decreases up to ^{9}Li and shows a sudden increase for ^{11}Li. Some models [7] which include nuclear correlations can explain the experimental data. Since the charge radii for Li isotopes include both 1s and 1p contributions, the 1p contribution might be the reason for the increase, due to the attractive

force between protons in the $1s_{1/2}$ core orbit and valence neutrons in $1p_{1/2}$ orbit. In such cases, independent measurements of the charge radius of the core gives additional important information for ^{11}Li.

In order to show that the (p,2p) reaction in inverse kinematics can be used to deduce reliable information on the charge radius of each orbit (or at least in the core) through the momentum distribution measurement, the best way is to measure the charge radius of the 1s orbit using the ^{3,4,6,8}He(p,2p) reaction and compare the results with those from laser spectroscopy. Once the method is established, measurements can be extended to $^{6-11}$Li isotopes for additional information on the charge radius of the inner shell, and heavier carbon isotopes as an extension of the $^{9-16}$C measurements. At this stage, it is very interesting to know at the same time how the neutron distribution in the core is modified in neutron-rich nuclei such as $^{6-8}$He. This can be done by (p,pn) neutron knockout reactions. Although not included in this proposal, the use of a neutron detector is discussed in section (2-7) as one of the future extensions.

In the HIMAC experiment, the separation energy resolution was about 1.3 MeV (rms). Although it is still enough for the charge radius measurements involving inner shell orbits, it is not sufficient to separate various final states for studying hole states in the valence orbit. The separation energy resolution can be improved by about a factor of two by minor modifications to the existing detectors. Although the resolution is still worse than γ-ray-tagging methods, the (p,2p) reaction can be used to study particle-unbound excited states such as in $^{23-24}$O and particle-unbound ground state in ^{25}O near N=16 region, where no particle-bound excited states are known to exist.

A broad-range forward magnetic spectrometer is used to detect the hole state or particles from the decay of the hole state. The usage of the magnetic spectrometer is essential in order to identify the production of the ground state and the deep-hole states. At RIBF the broad range spectrometer SAMURAI has been proposed and is under design. SAMURAI is the ideal spectrometer for these studies but it will unfortunately not be available within the next few years and so an intermediate solution must be found. The magnetic spectrometer we have used at HIMAC is limited to A < 15 due to the small bending power of the magnet. We therefore propose to install a forward magnetic spectrometer system with moderate bending power (BL= 2.2Tm) and gap (40cm) utilizing the secondhand C-type magnet available at KEK and available tracking detectors. The magnet, once installed at RIBF, can be used for invariant-mass spectroscopy of the particle-unbound final states by detecting particles, including projectile-rapidity neutrons, from the decay of the hole states. This method will in general provide better energy resolution near the threshold.

A beam energy around 250 MeV/A has been chosen, by considering the separation-energy resolution, opening-angle acceptance, nuclear reaction in the detector for stopping high-energy protons,

beam energy of the previous measurement and the primary beam energy at RIBF.

(2-2) **Goals**

(2-2-1) **Construction of the broad-range magnetic spectrometer**

The broad-range magnetic spectrometer will be constructed at the F12 area by combining the secondhand C-type magnet from KEK and available position detectors. The configuration of the system is shown in Fig. 2A. Preparing the power supply is the biggest problem.

(2-2-2) **Charge radius of the inner shell for He, Li, and C isotopes via ^{3,4,6,8}He(p,2p), ^{6,7,8,9,11}Li(p,2p), and ^{14,15,16,17,18}C(p,2p) reactions.**

^{3,4,6,8}He(p,2p) :

^{3,4,6,8}He(p,2p) reactions are used to measure the momentum distribution of inner-shell or core ($\pi 1s_{1/2}$) protons. The proton separation energy of He isotopes is shown in Fig. 2. Two protons are detected at laboratory angles around 41° with an angular coverage of $\pm 10^{\circ}$. From the width of the momentum distribution assuming a Gaussian shape, the rms charge radius of the inner-shell proton is deduced and compared with values obtained by laser spectroscopy [5]. These measurements are necessary to establish that the charge radius of the inner-shell can be deduced from the (p,2p) reaction.

^{6,7,8,9,11}Li(p,2p) :

^{6,7,8,9,11}Li(p,2p) reactions are used to measure the momentum distribution of inner-shell ($\pi 1s_{1/2}$) and valence ($\pi 1p_{3/2}$) protons. Protons are detected at laboratory angles around 41°, optimized for inner-shell protons. From the width of the momentum distribution of inner-shell protons assuming a Gaussian shape, the rms charge radius of the inner-shell proton is deduced and compared with the total charge radius from laser spectroscopy [6]. This measurement will also provide information on the energy gap between the 1s and 1p orbits, and which orbit contributes more to the increase of the total charge radius of ^{11}Li.

^{14,15,16,17,18}C(p,2p) :

^{14,15,16}C(p,2p) reactions will be re-measured by setting a proton detection angle at around 36°, optimized for 50MeV-bound 1s protons. Consistency of the separation-energy and momentum distributions with the previous measurement will be checked. Then the measurement is extended to heavier carbon isotopes ^{17,18}C. Of particular interest is the mass-number dependence of the energy gap between the 1s and 1p orbits, momentum distribution widths of 1s/1p protons, and the charge radius of the 1s protons.

(2-2-3) Ground and Excited States of ^{23,24,25}O

A topic of great interest in modern nuclear physics is the modification of shell structure with increasing isospin asymmetry. A particularly prominent example arises in the light neutron-rich nuclei where experimental evidence is accumulating that the N=20 shell closure is weakened and a new shell closure at N=16 appears. The mechanisms giving rise to this effect are poorly understood at present. Of crucial importance are studies of the structure of nuclei around the doubly magic nucleus ^{24}O and in particular the chain of Oxygen isotopes from the stability line up to and beyond the neutron dripline. Such studies are challenging because, for example, the isotopes ^{23,24}O are known to have no particle-stable excited states, and ^{25}O, which is the doubly-magic nucleus ^{24}O plus one neutron, is known to be particle unbound.

We propose to study the ground and excited states in ^{23,24,25}O by (p,2p) reactions from ^{24,25,26}F beams that can be produced with relatively high intensity. In order to improve the separation-energy resolution, a SHT target of 3mm thickness will be used, and PDC and NaI(Tl) detectors set far apart from the CVC. With a separation energy resolution of 0.4-0.6 MeV (rms), excited states corresponding to $\pi p_{3/2}^{-1}$, $\pi p_{1/2}^{-1}$, and $\pi s_{1/2}^{-1}$ can be observed in the doubly-magic nucleus ^{24}O. In order to complete our systematic study of the chain of Oxygen isotopes from stability to the neutron dripline, we would also propose to study the ^{19,21,23}F(p,2p)^{18,20,22}O reactions.
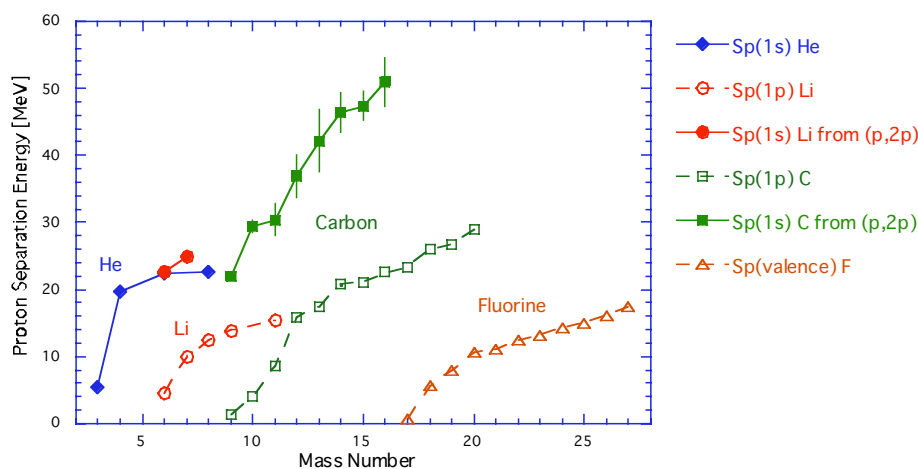

Fig. 2. Separation energy of valence/inner-shell protons for He, Li, C, and F isotopes

(2-2-4) The ^{17}Ne nucleus – possible candidate for a two-proton halo

Theoretical works [9,10] predict that ^{17}Ne could be the only realistic candidate to posses a two-proton halo. The condition for the existence of a halo in ^{17}Ne can be reasonably quantified in terms of s/d configuration mixing. Fig. 3, taken from [11], shows how the momentum distribution of the valence protons changes with varying assumptions about the s/d ratio in ^{17}Ne.

We propose a (p,2p) knock-out measurement for ^{17}Ne. The momentum distributions measured

for valence protons, corresponding to the population of four low-lying resonances in ^{16}F, will be quite sensitive to the halo structure of this nucleus, allowing one to make firm conclusions about the s/d configuration mixing.
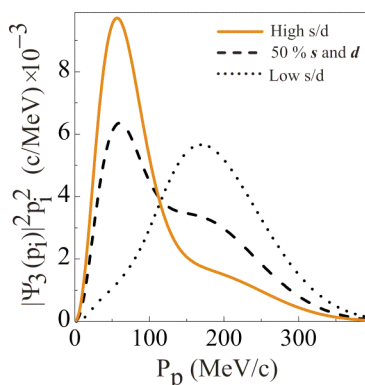

Figure 3. Momentum distributions of a valence proton in ^{17}Ne calculated taking different assumptions about the s/d mixing. The results are taken from Ref. [11].

[3] Experimental setup

(3-1) Detector system

The RI beam with an energy of 250 MeV/A is momentum tagged by an MWPC (WCB) placed at the momentum dispersive focal plane F5. An MWPC is used instead of PPAC's in order to detect proton, He and Li isotope beams. Momentum resolution is better than 0.1% (rms) estimated from a momentum dispersion of 3.3 cm/% at F5. Actual resolution will be worse since the tilt angle of the focal plane cannot be corrected for by a single position measurement. TOF and ΔE measurements are performed for particle identification by three plastic scintillators, SF8, SF12A, and SF12B, placed at two achromatic focal planes, F8 and F12. TOF between F8 and F12 with about 17 m of flight path may be enough for the present purpose.

The detector system for the (p,2p) measurements is placed at F12 area as shown in Fig. 4A, and the target region is expanded in Fig. 4B. A summary of the position detectors are shown in Table.1.

The beam vector on the target is measured by two sets of drift chambers (BDC1 and BDC2). The two sets are separated by about 1m with a He bag in between in order to have an angular resolution much less than 1 mrad. A beam veto scintillator (BV) with a 25mmϕ hole is placed between BDC1 and the target chamber for rejecting the beam halo hitting the copper block around the target.

The solid hydrogen target (SHT), with a thickness of 3-5mm, a diameter of 40mm and covered by two 9μm-thick aramid windows, will be used. It provides high S/N ratios of over 100 and is essential for the observation of the deep hole states. Entrance and exit windows for the beam and the exit

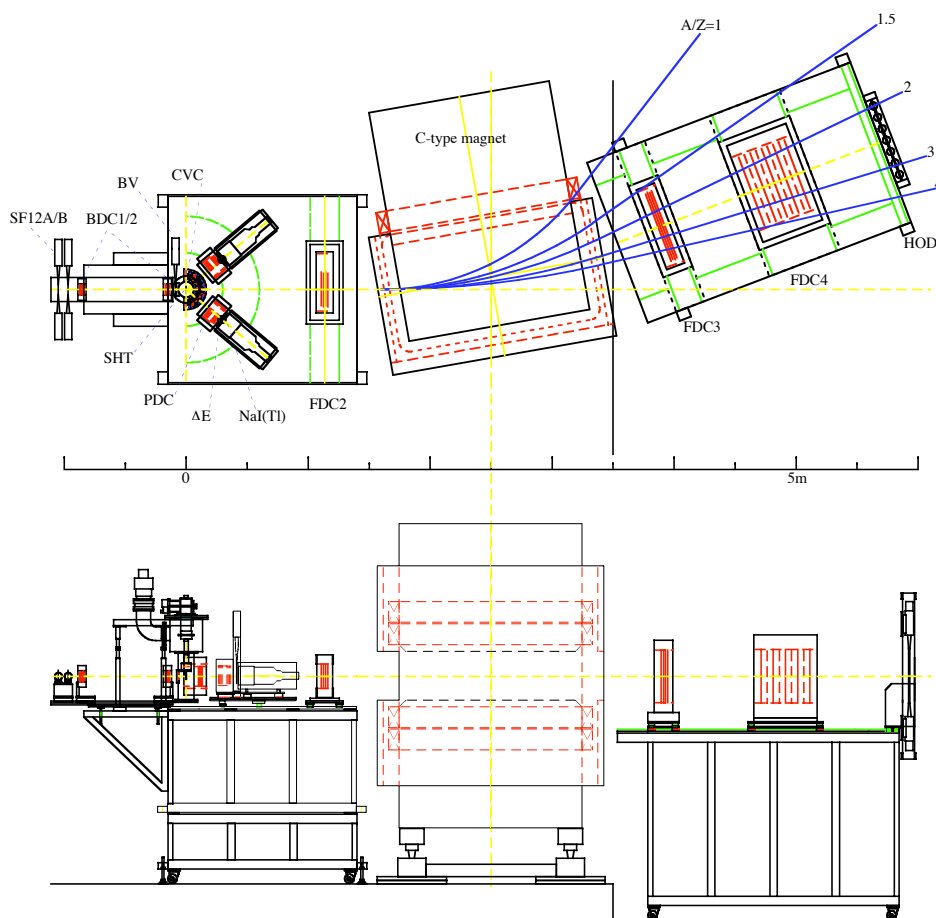window for the protons of the SHT vacuum chamber are made of 50μm-thick Kapton .
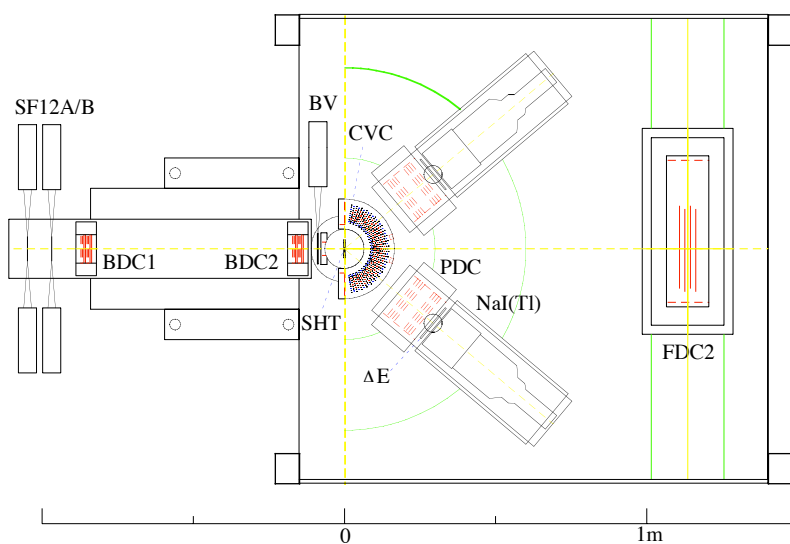

Fig. 4A : Experimental Setup at F12

Fig.4B : Expanded view of the setup around the target

Detector	Half cell [mm]	Cell type	Plane configuration	Effective area [mm]	#Readout channels	L/L_r [x10^{-3}]
WCB	2	MWPC	xx	240 x 150	64 x 2	1.0
BDC1	2.5	Walenta	xx'yy'xx'yy'	80 x 80	16 x 8	0.57
BDC2	2.5	Walenta	xx'yy'xx'yy'	80 x 80	16 x 8	0.57
FDC2	10.5	hexagonal	xx'xx'	242 x 160	12 x 4	0.39
FDC3	10.5	hexagonal	xx'xx'	558 x 400	28 x 4	0.43
FDC4	20	box, field shaping	xyx'y'xyx'y'x	600 x 400	16 x 9	2.7
CVC	~7	hexagonal	xx'xx'	half cylindrical	20 x 4	0.37
PDCL	10	Walenta	xx'yy'xx'yy'	140 x 140	8 x 8	0.67
PDCR	10	Walenta	xx'yy'xx'yy'	140 x 140	8 x 8	0.67
				Total #readout	896	

Table 1. Summary of position detectors

Protons emitted from the (p,2p) reaction are measured by two proton telescopes, consisting of a half-cylindrical vertex chamber (CVC), a proton drift chamber (PDC), a 5 mm-thick ΔE scintillator, and a 6"-diameter x 5"-thick NaI(Tl) scintillator. Telescopes are set at an optimum angle for each separation energy of interest: e.g. 39° for S_p= 30MeV. Angular acceptance is ±10° in both horizontal and vertical directions. Protons up to 210 MeV can be measured by 5"-thick NaI(Tl) detector with about 1% energy resolution.   Angular resolution of 1.5-2.0 mrad (rms) can be obtained by a combination of the CVC and PDC detectors. From the 4-momenta of the incident beam and the two outgoing protons, the separation energy and momentum of the knockout proton are obtained. Separation energy resolution is estimated to be about 0.5-0.7 MeV (rms), resulting from the accuracies of beam momentum tagging (<0.1%), the angular measurement for protons (1.5-2.0 mrad) including multiple Coulomb scattering in the target, and the energy measurement for protons (~1%).

The energy calibration of the NaI(Tl) detector will be performed by measuring p(p,2p) reactions using a 270 MeV secondary proton beams on SHT. The beam momentum is tagged by the WCB placed at F5. By setting the NaI(Tl) detectors at (34°,53°), (43°,43°), and (53°,34°), the detectors are calibrated between 50 MeV and 210 MeV.

The forward magnetic spectrometer is used to detect the hole state directly or particles from the decay of the hole state in order to measure the decay modes of the hole state. The system consists of a C-type magnet (Kappa), three sets of drift chambers (FDC2, FDC3, FDC4), and a scintillator hodoscope (HOD). The magnet provides a maximum field integral of BL= 2.2 Tm: projectiles of A/Z=3 at 250 MeV/A (R=2.2 GeV/c) can be bent by about 23°. The hodoscope consists of 7 slats of 1cm-thick plastic scintillators with transistorized bases for high rates, covering 70cm horizontally and 45 cm vertically. By filling the spaces between the FDC's with He bags, the momentum resolution will be better than 0.5% at 2.2 GeV/c. The high voltages of the FDC's have to be adjusted to

projectile fragments with smaller charges. The severest case is for the He isotope beams, where the FDC's have to be sensitive to fragments with Z=1. Due to the higher high voltage/gain and the limited segmentation of FDC's, the beam intensity will be limited to $< 3\text{-}5\text{x}10^5$/sec. Charge and mass of the fragments are identified by combining momentum, energy loss, and TOF measurements. For a TOF resolution of 0.1 nsec over a flight path of 6 m, 4σ mass separation is possible up to A=40, sufficient for the present measurement.

All the drift chambers, except the WCB, are operated using a He+50%C_2H_6 (L_r= 638m) gas mixture after bubbling through isopropyl alcohol.

(3-2) Detectors to be constructed

The position detectors WCB and CVC have to be constructed. All other detectors are already available.

WCB is a standard 2mm-spacing MWPC with 2 anode planes to increase the redundancy and the tracking efficiency. In order to reduce the number of readout channels, anode wires are read out in every 4mm. This configuration still gives sufficient momentum resolution. The chamber is filled with i-C_4H_{10} at low pressure in order to use relatively thin gas windows in the F5 vacuum chamber. A gas pressure of 200 Torr is necessary for the chamber to be sensitive to 300 MeV protons with 2 times minimum ionization. For He, Li, and F isotopes, the pressure can be reduced.

CVC is a half cylindrical drift chamber with 4 layers of hexagonal cells. In the previous experiment using PDC's, the angular resolution for protons was 3 mrad (rms), limited by the multiple Coulomb scattering in the target, the vacuum window (L/L_r= $1.7\text{x}10^{-4}$), 17cm of air (L/L_r=$0.6\text{x}10^{-3}$) and the angular resolution of the PDC. CVC provides an additional position measurement close to the target in a horizontal direction, and serves also as a He bag filled with He+50%C_2H_6. By combining the position information from the CVC and the PDC, the angular resolution will be improved by about a factor of two. Since the cell size is larger for the outer layers, the gain among layers will be adjusted by applying small amount of positive high voltage to anode wires, while all field wires are operated at common negative voltage.

(3-3) Electronics

The signals from the gas detectors are converted into LVDS signals by the ASD boards mounted on the detector. Power (±3V), threshold, and test pulses are supplied to the ASDs via twisted cables from PS modules in local NIM BINs. ASDs work stably at a threshold level corresponding to about 5 fC. At F5, the LVDS signals from the WCB are sent to TDC's in a local VME crate placed at F5. The VME controller signals are sent to DAQ-PC in a B3 counting area via optical fiber. High voltage to

the WCB is supplied from the local HV module controlled via a network for avoiding possible ground loop problems. At F12, LVDS signals are sent to TDC's in a local VME crate at F12. VME controller signals are also sent to the DAQ-PC in a B3 counting area via optical fiber. HV's (about 16) for gas detectors at F12 are supplied from B3. The number of electronics for the gas detectors are 56 ASD's, 7 ASD power supplies and 14 VME TDC's in 2 VME crates.

HV's for PMT's at F12 are supplied from the local HV module with remote control. Signals from PMT's are sent to local discriminators. The start scintillator at F8 may be a standard one supplied by the beam channel (?).

The reaction trigger is formed by SF12A*SF12B*SF12_window*ΔE_L*ΔE_R. Analog signals (SF12*4, SF12_sum*2, BV*1, ΔE*2 , NaI*2, HOD*14) are sent via BNC cables to B3. Logic signals from discriminators (SF8*2, SF12*8, BV*2, ΔE*4, NaI*4, HOD*15) are sent via twisted-pair cables to B3. The DAQ PC and CAMAC crate for the ADC's and TDC's are placed at B3. VME crates at F5 and F12 are connected to the DAQ-PC via optical fibers.

(3-4) Secondary beam parameters

The requirements for the secondary beam tuning are (1) constant beam energy at about 250 MeV/A for each isotope, (2) small beam spot on the SHT target, and (3) quick beam switching among different isotopes. Table 2 shows estimates of beam intensity using LISE++.

Primary beam	Energy [MeV/u]	Secondary beam	Energy [MeV/u]	Prod. Target [g/cm2]	Wedge @F1 [mm]	[mrad]	Wedge @F4 [mm]	[mrad]	B(D6) [T]	Intensity [/sec/100pnA]	Intensity to be used [/sec]	Measuring time / Isotope [hours]	Measuring time for Isotope chain [hours]
18O	350	p	270								1.0E+06	12	12
18O	350	3He	254	11.03	11	11.6			0.6144	8.83E+07	3.0E+05	10	40
		4He	252	8.99	42	47.6			0.8129	3.32E+07	3.0E+05	10	
		6He	253	6.93	95	123.7			1.2236	9.01E+06	3.0E+05	10	
		8He	251	8.12	110	144.2			1.6269	2.82E+05	3.0E+05	10	
18O	350	6Li	253	9.01	18	20.6			0.8167	1.09E+08	3.0E+05	10	53
		7Li	254	7.30	36	41.8			0.9528	8.80E+07	3.0E+05	10	
		8LI	253	7.19	43	49.9			1.0879	3.42E+07	3.0E+05	10	
		9LI	252	7.13	50	57.7			1.2221	8.31E+06	3.0E+05	10	
		11Li	252	5.45	86	105.0			1.4944	1.20E+05	2.4E+05	13	
22Ne	350	14C	246	5.77	14	18.0			0.9359	2.43E+08	3.0E+05	10	50
		15C	255	5.44	14	16.8			1.0221	6.32E+07	3.0E+05	10	
		16C	256	5.05	14	16.2	7.0	18.6	1.0799	1.23E+07	3.0E+05	10	
		17C	251	5.26	14	16.1	7.0	18.8	1.1484	1.81E+06	3.0E+05	10	
		18C	262	4.56	14	16.0	7.0	18.7	1.2478	2.09E+05	3.0E+05	10	
		19C	267	4.29	14	15.9	7.0	18.7	1.3307	2.13E+03			
22Ne	350	19F	259	0.90	20.0	24.7			0.8719	4.80E+08	3.0E+05	10	65
		21F	259	1.60	20.0	22.8			0.9621	5.71E+08	3.0E+05	10	
48Ca	350	23F	262	2.90	7.0	8.1			1.0611	2.32E+06	3.0E+05	10	
		24F	263	2.90	7.0	8.1			1.1098	3.90E+05	3.0E+05	10	
		25F	264	2.96	7.0	8.1			1.1577	5.96E+04	1.2E+05	25	
		26F	273	2.61	7.0	8.0			1.2276	7.44E+03			
20Ne	400	17Ne	253	7.25	7.4	8.9			0.6971	1.75E+07	3.0E+05	10	10
										Total measuring time [hours]			230

Table 2. Beam parameters and estimated measuring time

The target thickness and degrader thickness at F1/4 are optimized to have a maximum beam intensity at around 250 MeV/u starting from 350 MeV/A primary beams. For He and Li isotopes, the ^{18}O primary beam is optimum since the beam intensity from the ^{40}Ar or ^{48}Ca beams is quite low. For C isotopes, ^{22}Ne is optimum for the same reason. The Oxygen isotopes are produced from both ^{22}Ne and ^{48}Ca primary beams as the contamination of $^{23-26}$F beams produced from ^{48}Ca beams is relatively high.

Proton beams with 10^6/sec can be used for the energy calibration of the NaI(Tl) detectors, since the WCB and BDC's are used. If He, Li, C, and F runs are separated in time, we would like to have proton beams before each measurement for energy calibration. In most cases, a RI beam intensity higher than 10^6/sec can be obtained. But we would like to limit the actual beam intensities to below 3×10^5/sec for the drift chambers in the forward magnetic spectrometer. For ^{11}Li, ^{18}C, and ^{25}F beams, a primary beam intensity of 200 pnA is assumed. For the first round of experiments, we will use beams whose intensity is higher than 10^5/sec. In that sense, ^{19}C and ^{26}F will be omitted.

(3-5) Forward magnetic spectrometer

The central part of the forward magnetic spectrometer is a secondhand C-type magnet (Kappa) with moderate bending power and gap. The specification of the magnet is summarized in Table. 3.

Gap	0.4 m	#Turns	200
Pole	0.8m x 1.5m	Current	2300 A
Max. Field	1.2 T	Voltage	275 V
Effective length	1.8 m	Motive force	0.45 MAT
Max. BL	2.2 Tm	Power	580 KW
Weight	54 t	Cooling water	10 kg/cm^2, 150 l/min

Table 3 : Specification of the C-type magnet (Kappa)

The magnet will be borrowed from KEK. The power supply (2300A, 300V) for the magnet has to be prepared. Since a new power supply will cost about 30MY, we are considering the possibility to use one of the TARN II power supplies (output: DC 2500A, 600V, input: AC 3.3kV) borrowed from the mass ring project at KEK, until the mass ring comes into operation. The power supply is scheduled to be checked in this fiscal year.

The magnet will be placed at the most downstream part of the F12 area, so that the magnet will not interfere with other experiments. Since the original magnet was made for a beam height of 164.5cm, an additional iron plate of 5.5cm thick is necessary to be placed under the magnet stand. Charged particles are bent to the left side as shown in Fig. 6. This allows a neutron hodoscope for (p,pn) reactions to be incorporated in the setup in the future. There is also space in the forward direction for a future neutron hodoscope for invariant-mass spectroscopy in coincidence with

11

projectile-rapidity neutrons. The calculated magnetic field along the beam axis is shown Fig. 5. The fringing field is relatively strong due to the nature of the C-type magnet. In addition to the magnet installation, downstream detector stands have to be designed and constructed.
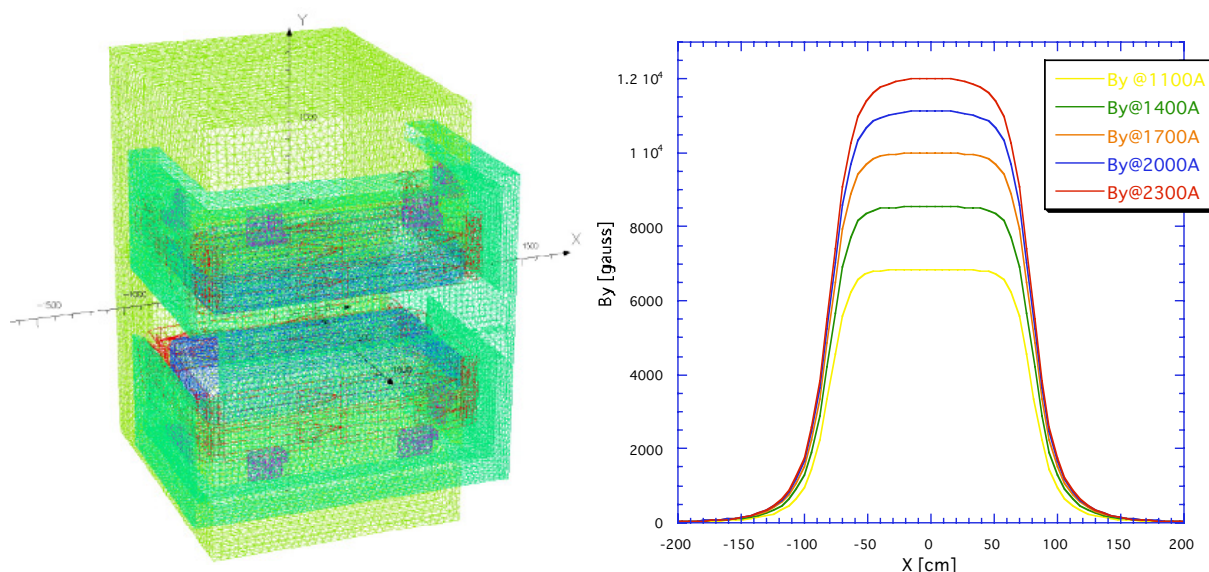

Fig. 5. C-type magnet (left) and calculated magnetic field (right)

(3-6) **Future option: Neutron hodoscope for (p,pn) reactions**

In addition to studying protons in the inner shell, it is very interesting to study also neutrons in the inner shell at the same time. This can be done by the (p,pn) neutron knockout reaction. Although not included in this proposal, we outline below a preliminary design of the neutron hodoscope for the (p,pn) reaction in the light-mass region, as one of the future extensions.
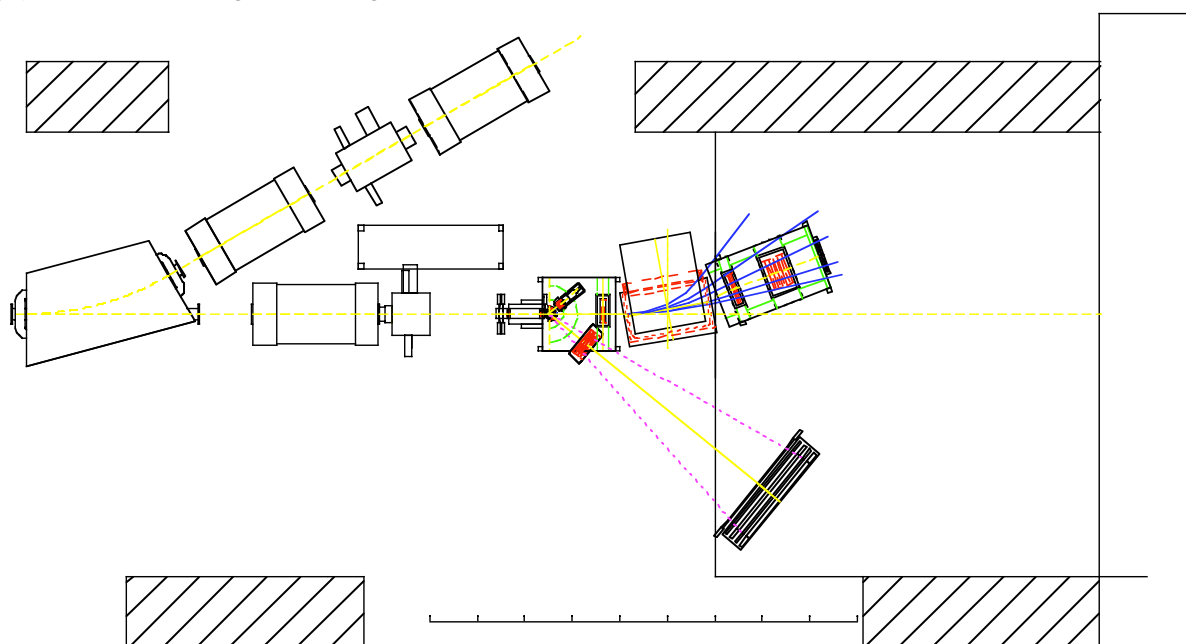

Fig. 6. Setup at F12 region including a neutron hodoscope as a future option for (p,pn) reactions

By combining existing plastic scintillator bars (32x 6cmx6cmx200cm, 32x 6.5cmx6.5cmx205cm) from the E4 and E6 experiments, a neutron hodoscope covering 200cm horizontal and 100cm vertical with 4 layers can be arranged. The total thickness is 25cm, providing about 25% detection efficiency. When placed about 6m away from the target, the angular coverage is $\pm9.5^o$ horizontally and $\pm4.8^o$ vertically. The angular resolution is about 3 mrad (rms) in both the horizontal and vertical directions. The estimated separation energy resolution is about 1.3 MeV (rms). This resolution will be enough to study inner shell neutrons in He or Li isotopes. By putting a drift chamber between the target and the neutron hodoscope, the (p,2p) reaction can be studied at the same time. A typical setup is shown in Fig. 6.

(3-7) Future option: Target recoil detector array development

The existing target recoil detectors are suited for initial experiments with the higher secondary beam intensities. However for future experiments, much larger solid angle coverages will be desirable. It is planned to use components of the target recoil detector arrays that are currently under development for the R3B/EXL collaborations at GSI/FAIR. These arrays combine a tracking detector composed of multiple layers of double-sided silicon microstrip and/or MAPS detectors, and a calorimeter detector composed of scintillating crystals such as CsI(Tl).

Tracking detectors: Si microstrip and MAPS detectors are under development at Daresbury and GSI, together with other groups in the R3B/EXL collaborations.
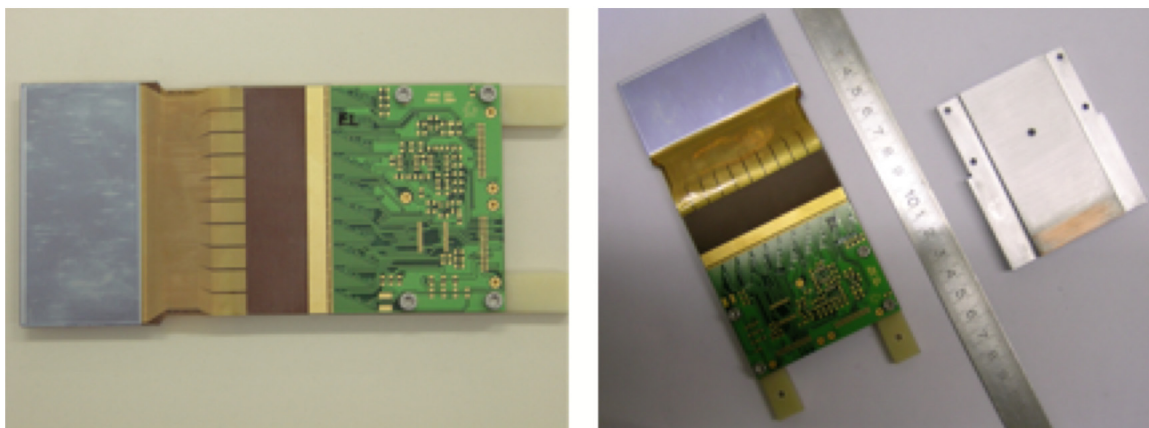

Figure 7. Double-sided silicon microstrip detectors developed by the R3B/EXL collaborations.

Detector area - 72×41.3 mm^2, thickness – 300 μm, 1024 strips per detector, with associated

ASIC-based readout electronics.

Initial simulations of the tracking detector have assumed two layers of double-sided silicon microstrip detector, with an active area of 70mm x 40mm. The first layer is 100μm-thick (L/L$_r$=1.1x10^{-3}) with 100μm-pitch. The second layer is 300μm-thick with 100μm-pitch which is separated from the first layer by 75mm, providing an angular resolution of about 2 mrad (rms). First prototypes of the silicon

microstrip detector for the second layer are shown in Fig. 7 and are presently being tested in-beam at GSI

Calorimeter detectors: CsI(Tl) detectors are under development at JINR, Dubna, as shown in Fig. 8. Source tests using 7.7 MeV alpha particles gave a measured energy resolution of 1.9-3.0% (FWHM), dependent on the crystal size. Crystals (with a size of $25x25x49mm^3$) have also been tested using a ^3H beam at 60 MeV/A and a measured energy resolution of 0.5% (FWHM) was achieved. At present 25 CsI crystals with a size of $25×25×50$ mm^3 are being manufactured in Dubna. Sixteen such crystals could be combined to form a $50x100x100mm^3$ detector viewed by 8 photodiodes. The detector fits well the Si microstrip Si detectors described above and protons up to 192 MeV can be measured.
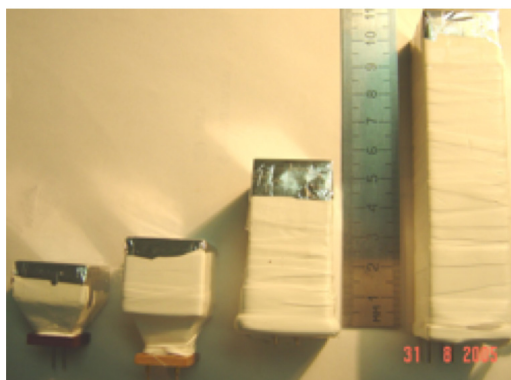

Figure 8. CsI detectors developed in Dubna. Crystal sizes are $25x25mm^2$ in cross section, and the thickness is 15, 25, 50, and 100mm.

[4] **Estimation of beam time**

We have estimated the necessary measuring time using estimated beam intensities in Table 2 and by scaling the statistics obtained in the HIMAC experiment. When the 5 mm-thick SHT is used, an integrated beam of 10^{10} gives sufficient statistics for momentum and separation-energy measurements. The necessary measuring time for isotopes with a beam intensity of $3x10^5$/sec is about 10 hours. The beam time estimate is also shown in Table. 2. The measuring time is 12 hours for protons, 40 hours for four He isotopes, 53 hours for five Li isotopes, 50 hours for five C isotope, 65 hours for five F isotopes, and 10 hours for ^{17}Ne. In addition, about 12 hours for electronics adjustment and about 8 hours for tuning the position detectors for each element (same Z) are necessary. Since the measuring time for each isotope is typically 10 hours, it is necessary to establish a method to switch beams in a short time. It is not clear how to install several degraders at F1. Since beam-switching time is not clear, it is not included in the estimate. If the He, Li, C, and F runs are separated in time, we would like to have some proton beam time for energy calibration at the beginning of each measurement.

[5] Readiness

Most detectors except the WCB and the CVC are available. An additional stand will be added below the existing stand to ensure that the beam/SHT/proton telescope will have the correct beam height as shown in Fig. 4A. When the problems of the magnet power supply are solved, the magnet will be transported from KEK and re-assembled and installed. The detector stand for the downstream detectors has to be designed and constructed. The WCB, the CVC, and the additional stand will be ready before the winter of 2007.

[6] References

1.   G. Jacob and Th.A.J. Maris, Rev. Mod. Phys. **38**, 121 (1966), Rev. Mod. Phys. **45**, 6 (1973).

2.   I. Tanihata et al., Phys. Rev. Lett. **55**, 2676 (1985), Phys. Lett. **B289**, 261 (1992).

3.   A. Ozawa, T.Suzuki, I.Tanihata, Nucl. Phys. **A 693**, 32-62 (2001).

4.   S.R. Neumaier et al., Nucl. Phys. **A 712**, 247 (2002) ; A.V. Dobrovolsky et al., Nucl. Phys. **A 766**, 1 (2006).

5.   L.B. Wang et al., Phys. Rev. Lett. **93**, 142501 (2004).

6.   G. Ewald et al., Phys. Rev. Lett. **93**, 113002 (2004) ; R. Sanchez et al., Phys. Rev. Lett. **96**, 033002 (2006).

7.   K. Varga, Y. Suzuki, and R.G. Lovas, Phys. Rev. **C66**, 041302 (2002).

8.   P.G. Hansen and J.A. Tostevin, Ann. Rev. Nucl. Sci. **53**, 219-261 (2003).

9.   M.V. Zhukov and I.J. Thompson, Phys. Rev. **C52**, 3505 (1995).

10.   L.V. Grigorenko, I.G. Mukha, and M.V. Zhukov, Nucl. Phys. **A713**, 372 (2003); Nucl. Phys. **A740**, 401(E) (2004).

11.   L.V. Grigorenko, Yu.L. Parfenova, and M.V. Zhukov, Phys. Rev. **C71**, 051604(R) (2005).